Angewandte Chemie
Eine Zeitschrift der Gesellschaft Deutscher Chemiker

Supporting Information

69451 Weinheim, Germany

Unprecedented Tetranuclear Complexes with 20 electron Ni^{II} Centers: The Role of Pressure and Temperature on Their Solid State and Solution Fragmentation

Anthony Kermagoret, Roberto Pattacini, Patricia Chavez Vasquez, Guillaune Rogez, Richard Welter and Pierre Braunstein*

[*] Dr. P. Braunstein, A. Kermagoret, Dr. R. Pattacini, P. Chavez Vasquez
Laboratoire de Chimie de Coordination, Institut de Chimie, UMR 7177 CNRS, Université Louis Pasteur
4 rue Blaise Pascal, 67070 Strasbourg Cedex, France.
E-mail: braunstein@chimie.u-strasbg.fr
http://www-chimie.u-strasbg.fr/~lcc/

Dr. G. Rogez
Groupe des Matériaux Inorganiques, IPCMS, UMR 7504 CNRS,
23, rue du Loess, B.P. 43
67034 STRASBOURG Cedex 2, France

Prof. R. Welter
DECOMET, Institut de Chimie, UMR 7177 CNRS, Université Louis Pasteur
4 rue Blaise Pascal, 67070 Strasbourg Cedex, France.

Experimental

1. General Considerations

All manipulations were carried out under inert dinitrogen atmosphere, using standard Schlenk-line conditions and dried and freshly distilled solvents. The ^1H, $^{13}C\{^1H\}$, and $^{31}P\{^1H\}$ NMR spectra were recorded unless otherwise stated on a Bruker Avance 300 instrument at 300.13, 75.47 and 121.49 MHz, respectively, using TMS, or H_3PO_4 (85% in D_2O) as external standards with downfield shifts reported as positive. FT-IR spectra in the range of 4000-650 cm^{-1} were recorded on a Nicolet Nexus FT-IR spectrometer coupled with a Continuum microspectrometer, operating in diffuse reflectance. Elemental C, H, N analyses were performed by the "Service de microanalyses", Université Louis Pasteur, Strasbourg. The solid state visible spectrum of **1a** was recorded on a CCD detector using a Nikon TE microscope (40 X; N.A. 0.45) and decomposed by an Acton/Princeton Instruments monochromator. The variable temperature spectra of **1a/b** were recorded on a VARIAN Cary05E, equipped with a OXFORD INSTRUMENTS DN1704 cryostat. Mass spectra were recorded with a Bruker Daltonics microTOF [ESI(+) capillary voltage: 4.8 kV; nebulizer pressure: 0.2 Bar; desolvation temperature: 180 °C; desolvation gas flow rate: 30 L/h]. Magnetic measurements were performed at the Institut de Physique et Chimie des Matériaux de Strasbourg (UMR CNRS-ULP 7504) using a Quantum Design MPMS-XL SQUID magnetometer. The susceptibility measurement was performed in the 300-1.8 K temperature range with an applied field of 5 kOe. Magnetization measurements at different fields at room temperature confirm the absence of ferromagnetic impurities. Data were corrected for the sample holder and diamagnetism was estimated from Pascal constants. 2-[(diphenylphosphino)methyl]oxazoline (PN_{ox}) was prepared according to literature procedures.[S-1] Anhydrous $NiCl_2$ was prepared by dehydration of $NiCl_2{\cdot}6H_2O$ at 150°C under vacuum prior to use. Other chemicals were commercially available and used as received.

2. Synthesis

2.1. Preparation and Spectroscopic Data for 2-[(diphenylphosphino) methyl]thiazoline (PN_{th}).

20 mL (32.0 mmol) of a 1.6 M *n*-BuLi solution was added dropwise to a solution of liquid 2-methyl-2-thiazoline (3.06 mL, 3.23 g, 32.0 mmol) in 100 mL of THF at –78 °C. The pale red reaction mixture was stirred for 1 h at –78 °C. Pure Me_3SiCl (8.09 mL, 6.95 g, 64.0 mmol) was then added dropwise and stirring was continued at -78 °C for 2 h. Pure PPh_2Cl (5.89 mL, 7.06 g, 32.0 mmol) was added dropwise to the colourless solution at –78 °C. The reaction mixture was allowed to reach at room temperature overnight. The volatiles were removed under reduced pressure, resulting in a yellow oily crude product which was dissolved in CH_2Cl_2 (50 mL). LiCl was removed by filtration. The solvent was evaporated, yielding pure PN_{th} as a pale yellow powder. Yield: 7.03 g, 68%. ^1H NMR ($CDCl_3$) **δ**: 3.25 (t, 2H, $^3J_{H-H}$ = 8.4 Hz, SCH_2), 3.32 (s, 2H, PCH_2), 4.14 (tt, 2H, $^3J_{H-H}$ = 8.4 Hz, $^5J_{H-H}$ = 0.7 Hz, NCH_2), 7.32-7.48 (m, 10H, aromatic). $^{13}C\{^1H\}$ NMR ($CDCl_3$) **δ**: 34.6 (d, $^4J_{P-C}$ = 2.0 Hz, SCH_2), 35.1 (d, $^1J_{P-C}$ = 17.1 Hz, PCH_2), 64.5 (s, NCH_2), 128.5-137.6 (m, aromatic, PPh_2), 167.7 (d, $^2J_{P-C}$ = 12.2 Hz, C=N). $^{31}P\{^1H\}$ NMR ($CDCl_3$) **δ**: -15.5 (s). Anal. Calcd. for $C_{16}H_{16}NPS$ (285.34): C, 67.35; H, 5.65; N, 4.91. Found: C, 67.06; H, 5.94; N, 4.99.

2.2 Preparation and Spectroscopic Data for $[Ni(PN_{th})Cl_2]_4$ (1a).

Solid **1b** (0.73 g, 1.75 mmol, see below) was dissolved in a minimum amount of CH_2Cl_2 and petroleum ether was quickly added (three times the volume of CH_2Cl_2). **1a** precipitated as a pale green powder. Yield: 0.71 g, 98%. FTIR (cm^{-1}) selected absorptions: 3071w, 3058w, 3038w, 3005w, 2984w, 2947w, 2932w, 2919w, 2904w, 2887w, 20870w, 2859w, 2854w, 1603vs, 1585m(sh), 1572m, 1483s, 1434s, 1397w(sh), 1382s, 1342w, 1324w, 1315w, 1277w, 1254m(sh), 1238s, 1190w, 1183w(sh), 1169w, 1159w, 1137w, 1128w, 1100s, 1093s(sh), 1071w, 1028vs, 1024vs(sh), 1004m(sh), 984w(sh), 949m, 907w, 862w, 853w, 841w, 827m(sh), 820m, 770m(sh), 764m(sh), 754m(sh), 739vs, 693vs, 690vs(sh), 672m. Anal. Calcd. for $C_{64}H_{64}N_4Cl_8Ni_4P_4S_4$ (M = 1651.8): C, 46.49; H, 3.90; N, 3.39. Found: C, 46.13; H, 3.66; N, 3.40.

2.3 Preparation and Spectroscopic Data for [Ni(PN_{th})Cl_2] (1b).

A solution of PN_{th} (0.51 g, 1.8 mmol) in methanol (10 mL) was added to a solution of $NiCl_2$ (0.23 g, 1.8 mmol) in methanol (100 mL), resulting in a green reaction mixture. Stirring was continued for 1 h at room temperature. The volatiles were removed under reduced pressure and the green solid obtained was left under vacuum for 12 h, yielding **1b** as a red amorphous solid. Yield: 0.73 g, 1.75 mmol, 98%. FTIR (cm^{-1}) (see Figure S-1) selected absorptions: 3051w, 2986w, 2947w, 2905w, 2861w, 1603vs, 1483m, 1435vs, 1386m, 1315w, 1275w, 1240s, 1189w, 1159w, 1100s, 1029vs, 1000w, 948w, 821w, 741vs, 693vs. ESI$^+$: $[M-Cl]^+$ 377.9779 (calcd. For $[C_{16}H_{16}NClNiPS]^+$: 377.9778). Anal. Calcd. for $C_{16}H_{16}NCl_2NiPS$ (M = 412.9): C, 46.49; H, 3.90; N, 3.39. Found: C, 46.07; H, 3.91; N, 4.23.

2.4 Preparation and Spectroscopic Data for [Ni(PN_{ox})Cl_2]$_4$ (2a).

Complex **2b** (1.20 g, 3.0 mmol, see below) was dissolved in a minimum amount of CH_2Cl_2 and petroleum ether was quickly added (three times the volume of CH_2Cl_2). **2a** precipitated as a pale green powder. Yield: 1.10 g, 92%. Alternatively **2a** can be obtained by evaporating under vacuum, and at ca. -15 °C, a solution of **2b** in a 2:1 CH_2Cl_2/heptane mixture. Yield: 1.18 g, 98%. FTIR (cm^{-1}) (see Figures S-2, S-3) selected absorptions: 3076w, 3058w, 3035w, 2991w, 2960w, 2933w, 2901w, 1667vs(sh), 1663vs, 1585w, 1574w, 1485s, 1475m, 1454w, 1442m(sh), 1438s(sh), 1434s, 1401s, 1372s, 1334m, 1270vs(sh), 1265vs, 1231w, 1199w, 1190w, 1166s, 1148w, 1104s, 1095w(sh), 1071w, 1045s, 1036s, 999m, 970w, 965w(sh), 938m, 926m, 820w, 814w, 752m(sh), 744vs, 737vs, 704m(sh), 695vs, 688vs(sh). Anal. Calcd. for $C_{64}H_{64}N_4Cl_8Ni_4P_4O_4$ (M = 1587.8): C, 48.37; H, 4.06; N, 3.53. Found: C, 48.29; H, 3.88; N, 3.65.

2.5 Preparation and Spectroscopic Data for [Ni(PN_{ox})Cl_2] (2b).

A solution of PN_{ox} (1.66 g, 6.2 mmol) in methanol (10 mL) was added to a solution of $NiCl_2$ (0.80 g, 6.2 mmol) in methanol (50 mL), resulting in a green reaction mixture. Stirring was continued for 1 h at room temperature. The volatiles were removed under reduced pressure and the green solid obtained was left under vacuum for 12 h, yielding **2b** as a red amorphous solid. Yield: 2.40 g, 97%. FTIR (cm^{-1}) (see Figures S-2, S-3) selected absorptions: 3054w, 2985w, 2914w, 1654vs, 1622vs(sh), 1484s, 1435vs, 1403s, 1371s, 1355m, 1268vs, 1190w(sh), 1169m, 1135w, 1101m, 1072w, 1029m, 999m, 971w, 931m, 829m, 742s, 693s, 665w. ESI$^+$: $[M-Cl]^+$ 3619984 (calcd. For $[C_{16}H_{16}NClNiPO]^+$: 362.0006). Anal. Calcd. for $C_{16}H_{16}NCl_2NiPO$ (M = 397.0): C, 48.37; H, 4.03; N, 3.53. Found: C, 47.93; H, 4.31; N, 3.69.

2.6 Preparation and Spectroscopic Data for $[Ni(PN_{th})Br_2]$ (3).

A solution of solid PN_{th} (0.86 g, 3.0 mmol) in 5 mL of methanol was added to a solution of $NiBr_2$ (0.66 g, 3.0 mmol) in 40 mL of methanol and the resulting dark red solution was stirred for 1 h at room temperature. Evaporation of the volatiles under reduced pressure yielded a deep red residue which was dissolved in 30 mL of CH_2Cl_2. $NiBr_2$ was filtered off and a red powder was precipitated with petroleum ether (80 mL). Drying under vacuum yielded **3** as a ruby red powder. Yield: 1.39 g, 2.8 mmol, 92%. FTIR (cm^{-1}): (see Figure S-1) selected absorptions: 3052w, 2926w, 2883w, 1600m, 1558s, 1483w, 1435vs, 1382m, 1310w, 1249m, 1186w, 1160w, 1103s, 1039m, 1029m(sh), 998w, 962w, 835w, 787w, 747vs, 736vs(sh), 689vs, 672m(sh). Anal. Calcd. for $C_{16}H_{16}NBr_2NiPS$ (M = 503.84): C, 38.14; H, 3.20; N, 2.78. Found: C, 37.89; H, 3.25; N, 2.51.

2.7 Preparation and Spectroscopic Data for $[Ni(PN_{ox})Br_2]$ (4).

Complex **4** was prepared following the same procedure described above for the synthesis of **3**, using PN_{ox} (0.61 g, 2.3 mmol) and $NiBr_2$ (0.50 g, 2.3 mmol). **4** was obtained as a deep red powder. Yield: 1.00 g, 2.05 mmol, 89%. FTIR (cm^{-1}) selected absorptions: 3066w, 2954w, 2911w, 1628vs, 1587w, 1573w, 1478m, 1453w, 1435vs, 1426s(sh), 1370m, 1339m, 1312w, 1268s, 1198w, 1178m, 1160w, 1133w, 1100s, 1071w, 1047m, 1027m(sh), 998m, 974w, 928m, 829m, 752m(sh), 742s, 712w(sh), 690s. Anal. Calcd. for $C_{16}H_{16}NBr_2NiPO$ (M = 487.78): C, 39.40; H, 3.31; N, 2.87. Found: C, 39.10; H, 3.56; N, 2.88

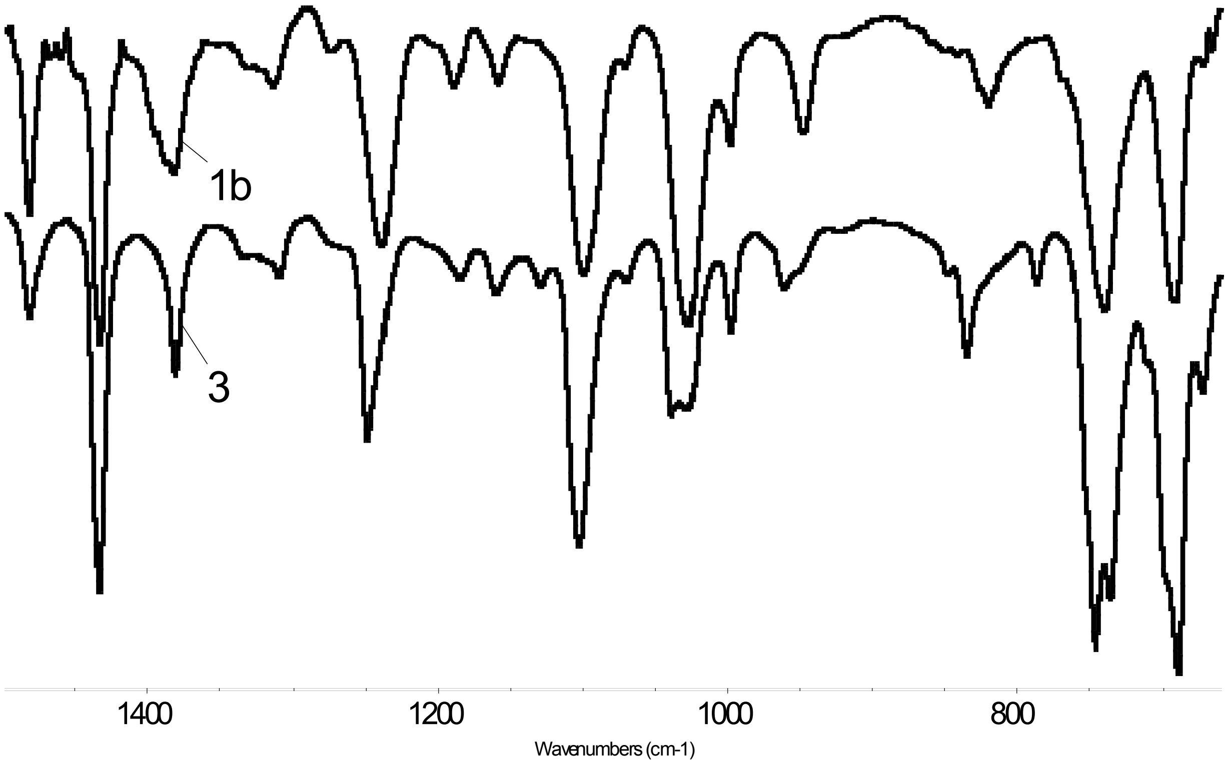

Figure S-1. Comparison between the FTIR spectra of **1b** and **3**, emphasizing the spectroscopic similarity between the two complexes.(reflectance mode, 1500-650 cm^{-1} region).

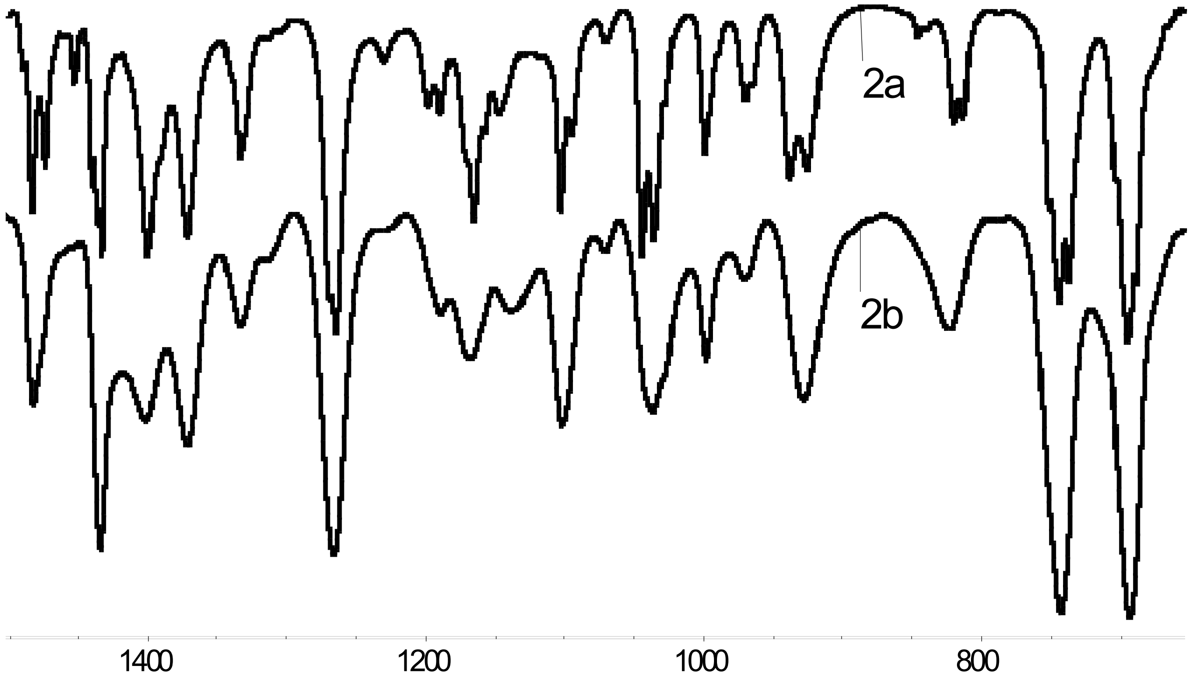

Figure S-2. Comparison between the FTIR spectra of **2a** and **2b** (reflectance mode, 1500-750 cm^{-1} region).

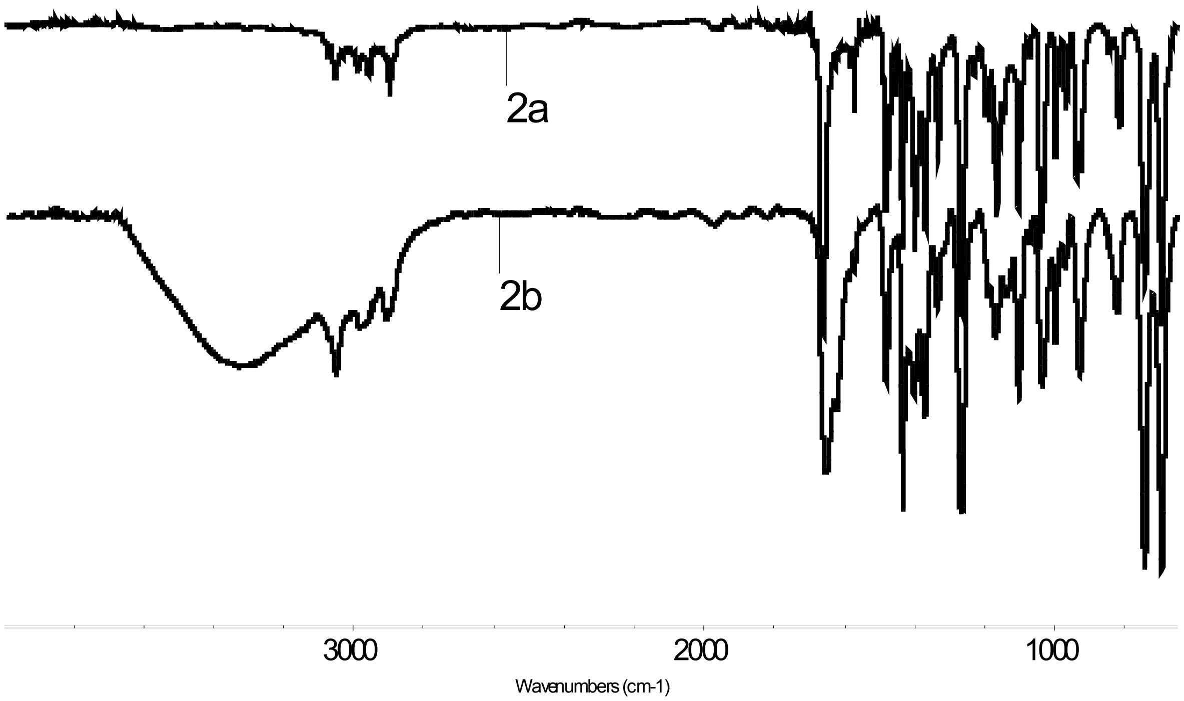

Figure S-3. FTIR spectrum (4000-650 cm^{-1} region) of **2a** (upper spectrum) recorded by FTIR microscopy immediately after isomerization from dry **2b** (lower spectrum) on a metallic support, with the aid of a spatula. The 3320 cm^{-1} absorption emphasizes its hygroscopicity.

3. Evans method[S-2]

A solution of paramagnetic species in CD_2Cl_2 (5 mg in 0.3 mL) was placed in a NMR tube and an inner narrow-bore NMR tube, containing a solution of CH_3NO_2 (20% Vol.) in CD_2Cl_2, was installed. The ν_{CH3} (Hz) is measured by ^{1}H NMR on a Bruker Avance 300 MHz instrument operating at 300.13 MHz, respectively, using TMS as external standard. $\nu°_{CH3}$ is measured in the same way, using pure CD_2Cl_2 instead of the sample solution. The simplified mathematic formula (1) is used to calculate the mass susceptibility χ_p which can was used to calculate the magnetic moment μ in Bohr Magnetons (BM) with formula (2).

(1) $\chi_p = \chi_0 + (3000.\Delta\upsilon)/(4\Pi.\upsilon_0.C.M)$

[$\chi_0 = \chi_{CD2Cl2} = -0.58 \cdot 10^{-6}$ (cm^3/l); ν_0 = 300013 Hz; $\Delta\nu = \nu_{CH3} - \nu°_{CH3}$; C = Concentration of the paramagnetic compound (mol/l); M = Molar mass of the paramagnetic compound (g/mol)]

(2) $\mu = 2.84 \cdot \sqrt{(\chi_p \cdot M \cdot T)}$

[T = Temperature].

4. Magnetic Study

The magnetic properties of **2a** were investigated in the 300-1.8 K temperature range with an applied field of 5 kOe. The Curie constant C = 4.64 emu•K•mol^{-1}, determined from the fit of the $1/\chi$ = f(T) curve with the Curie-Weiss law in the high temperature region (150-300 K), is in accordance with what is expected for four octahedral Ni^{II} ions (with a g value of 2.15).[S3]

Upon cooling, the χT product exhibits a regular decrease from 4.54 emu•K•mol^{-1} at 300 K to 3.47 emu•K•mol^{-1} at 20 K, indicating the occurrence of at least one intramolecular antiferromagnetic interaction. Below 20 K, the small increase of the χT product up to 3.49 emu•K•mol^{-1} at 14 K and the final decrease below 14 K are most probably due to the complicated interaction scheme and to the presence of competing intramolecular interactions (Figure S-4) as well as zero-field splitting and intermolecular interactions.

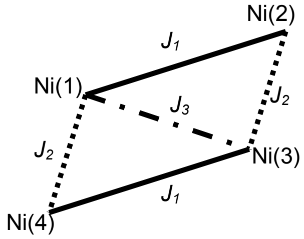

Figure S-4. Spin and interaction topology considered for Ni$_4$.

Considering the spin topology described in Figure S-5 and assuming each pairwise interaction is describable in terms of the Heisenberg Hamiltonian of the form $\hat{H} = -J_{ij}\,\hat{\mathbf{S}}_i \cdot \hat{\mathbf{S}}_j$, the complete spin Hamiltonian for Ni$_4$ is given in eq. 1:

$$\hat{\mathbf{H}} = -J_1\,\hat{\mathbf{S}}_1 \cdot \hat{\mathbf{S}}_2 - J_2\,\hat{\mathbf{S}}_1 \cdot \hat{\mathbf{S}}_4 - J_3\hat{\mathbf{S}}_1 \cdot \hat{\mathbf{S}}_3 - J_2\,\hat{\mathbf{S}}_2 \cdot \hat{\mathbf{S}}_3 - J_1\,\hat{\mathbf{S}}_3 \cdot \hat{\mathbf{S}}_4 \qquad (1)$$

As explained by Griffith and by Hendrickson, the existence of three different exchange constants for this peculiar spin topology prevents the use of the Kambe vector-coupling approach.[S4,S5,S6] Unfortunately, in the present case, no analytical fitting by full diagonalization of the complete spin Hamiltonian was successful in the whole temperature range. This may infirm the hypothesis of Heisenberg type interactions.

The magnetic properties of this compound require further studies, for instance by neutron diffraction, neutron scattering, or high-field EPR spectroscopy, in order to determine the amplitude and sign of the different exchange constants and the characteristics of the ground state (spin value, anisotropy).

5. Crystallography

5.1 X-ray data collection, structure solution and refinement for compounds 1a·2CH$_2$Cl$_2$, 3 and 4.

Suitable crystals for X-ray analysis of compounds **1a**·2CH$_2$Cl$_2$, **3** and **4** were obtained by layering hexane on dichloromethane solutions. The intensity data was collected at 173(2) K on a Kappa CCD diffractometer[S-7] (graphite-monochromated MoK$_\alpha$ radiation, λ = 0.71073 Å). Crystallographic and experimental details for the structures are summarized in Table S-1. An ORTEP plot of the molecular structure of **1a** in **1a**·2CH$_2$Cl$_2$ is shown in Figure S-5.

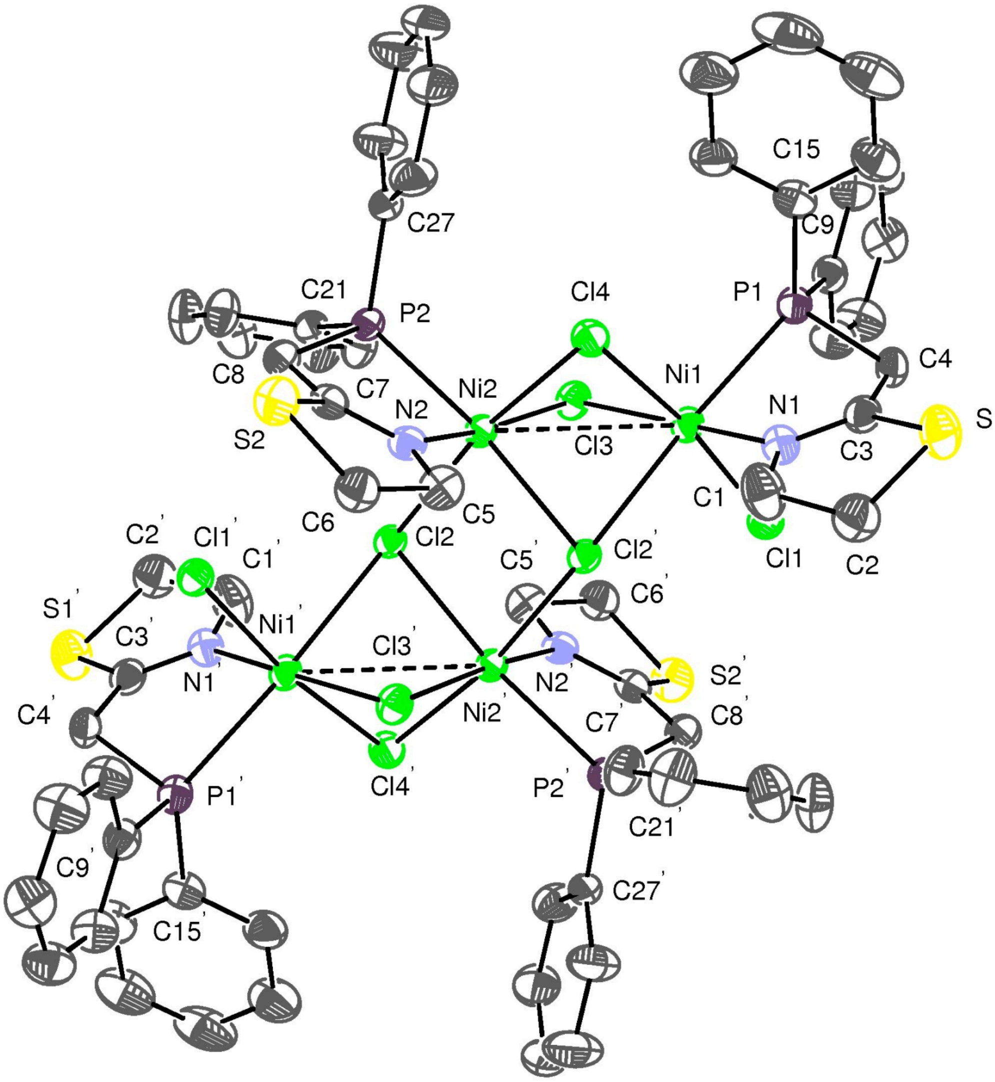

Figure S-5: ORTEP plot of the molecular structure of **1a** in **1a**·$2CH_2Cl_2$ together with partial numbering scheme. Ellipsoids include 30% of the electron density. Hydrogen atoms and solvent molecules are omitted for clarity.

The structures were solved by direct methods (SHELXS-97) and refined by full-matrix least-squares procedures (based on F^2, SHELXL-97)[S-7] with anisotropic thermal parameters for all the non-hydrogen atoms. The hydrogen atoms were introduced into the geometrically calculated positions and refined *riding* on the corresponding parent atoms. For **1a**, C2 and C6 were found disordered in two positions with equal occupancy factors and their position was refined isotropically. CCDC-641489 (**3**), 641490 (**4**) and 641491 (**1a**·$2CH_2Cl_2$) contain the supplementary crystallographic data that can be obtained free of charge via www.ccdc.cam.ac.uk/conts/retrieving.html (or from the Cambridge Crystallographic Data Centre, 12 Union Road, Cambridge CB2 1EZ, UK; fax (+44)1223-336-033 or deposit@ccdc.cam.ac.uk). Figure 1 was produced using the UCSF Chimera package from the Computer Graphics Laboratory, University of California, San Francisco: C.C. Huang, G.S. Couch, E.F. Pettersen, T.E. Ferrin, "Chimera: An Extensible Molecular Modeling Application Constructed Using Standard Components." *Pacific Symposium on Biocomputing* **1996**, *1*, 724.

Table S-1: X-ray data collection and refinement parameters for compounds **1a**·$2CH_2Cl_2$, **3** and **4**.

Compound	**1a·$2CH_2Cl_2$**	**3**	**4**
Formula	$C_{64}H_{64}Cl_8$ $N_4Ni_4P_4S_4 \cdot 2CH_2Cl_2$	$C_{16}H_{16}NSPNiBr_2$	$C_{16}H_{16}NOPNiBr_2$
FW	1829.60	503.86	503.86
Crystal System	Triclinic	Triclinic	Triclinic
Space Group	*P-1*	*P-1*	*P-1*
a, Å	11.248(1)	8.6595(3)	8.6330(3)
b, Å	11.518(1)	8.6983(2)	8.7360(3)
c, Å	14.843(2)	12.9457(4)	11.8890(4)
α, °	91.811(3)	91.476(1)	104.2010(17)
β, °	94.041(3)	98.175(1)	96.7060(17)
γ, °	97.161(3)	111.337(1)	96.3230(12)
V, $Å^3$	1901.6(3)	895.86(5)	854.28(5)
Z	1	2	2
D_{calcd}, g cm^{-3}	1.598	1.868	1.896
F(000)	932	496	480
Crystal size (mm)	0.14 × 0.14 × 0.10	0.10× 0.10 × 0.10	0.12 × 0.11 × 0.10
μ, cm^{-1}	1.634	5.74	5.90
Rflns. collected	17720	6954	6589
Rflns. unique	10978	4612	4548
Rflns. observed [$I > 2\sigma(I)$]	7468	3318	2768
Parameters	420	199	199
R Indices [$I>2\sigma(I)$]	*R1* = 0.0485 *wR2* = 0.1107	*R1* = 0.0438, *wR2* = 0.0965	*R1* = 0.0464, *wR2* = 0.0985
R Indices (all data)	*R2* = 0.0858, *wR2* = 0.1263	*R1* = 0.0743, *wR2* = 0. 1089	*R2* = 0.0999, *wR2* = 0.1194

5.2. X-ray powder data collection and cell refinement for compound 2a. Density estimation of 2a and 2b.

Powder X-Ray data for **2a** were obtained by using a Bragg-Brentano Siemens D5000 (CuKα1, λ = 1.54051 Å) diffractometer equipped with a primary beam monochromator. The cell parameters were determined with the program DICVOL04[S-8] and refined by profile fitting procedures with the program Fullprof2000.[S-9] The experimental and calculated diffraction profiles are depicted in Figure S-6, together with the trace of their difference (measured—calculated). Refined cell parameters: a = 11.379(4), b = 11.945(3), c = 15.479(5) Å, α = 83.58(3), β = 84.84(3), γ = 88.02(3)°, V = 2081(1) Å^3. Fitting refinement parameters: Bragg R: 0.0362, R_f = 0.04; χ^2: 1.22 GoF: 1.1.

The refined volume of V = 2081(1) Å^3 for **2a** results in a calculated density of 1.41 g/cm^3 when considering **2a**·2CH_2Cl_2 as the cell content. Co-crystallized CH_2Cl_2 was not detected in the powders of **2a** dried under vacuum and used for the powder X-ray diffraction analysis. The density for **2a** without cocrystallization solvent would then be estimated at 1.29 g/cm^3. The density of 1.55 g/cm^3, estimated for **2b** is calculated by considering that its cell volume is similar to that of **4** [854.28(5) Å^3]. The role of the solvent becomes clearer in the case of the **1a**/**1b** couple. The density of solid **1a**·2CH_2Cl_2 determined by single crystal X-ray diffraction as 1.60 g/cm^3, is higher than that estimated for **1b** (1.54 g/cm^3) and therefore incompatible with a pressure induced isomerization process. However, loss of CH_2Cl_2 from solid **1a**·2CH_2Cl_2 lowers its density to 1.45 g/cm^3, which is lower than that of **1b.** The Δd of the **2a** → **2b** isomerization is 0.31 g/cm^{-1} and it is higher than that of the **1a** → **1b** one (0.09 g/cm^{-1}), consistent with the higher pressure required for the latter process.

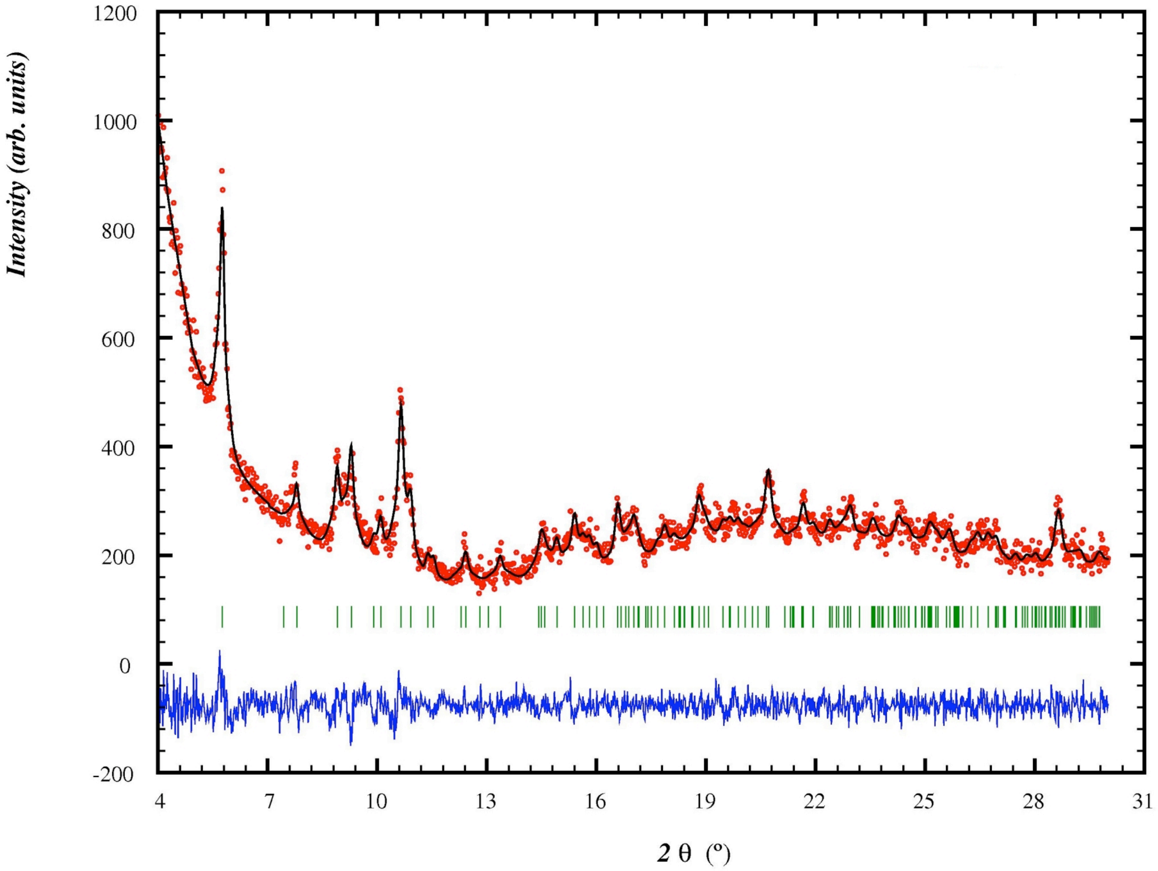

Figure S-6: Superimposition of the experimental (red dots) and fitted (black line) X-ray diffractions patterns of compound **2a**. The difference trace is reported in blue. Bragg positions are reported in green.

References

[S-1] P. Braunstein, M. D. Fryzuk, M. Le Dall, F. Naud, S. J. Rettig, F. Speiser, *Dalton Trans.* **2000**, 1067-1074.

[S-2] a) D. F. Evans, *J. Chem. Soc. (A)* **1959**, 2003-2005; b) S. K. Sur, *J. Magn. Res.* **1989**, *82*, 169-173.

[S-3] R. L. Carlin, *Magneto-chemistry*, Springer-Verlag, Berlin, **1986**.

[S-4] K. Kambe, *J. Phys. Soc. Japan*, **1950**, *5*, 48.

[S-5] J. K. McCusker, J. B. Vincent, E. A. Schmitt, M. L. Mino, K. Shin, D. K. Coggin, P. M. Hagen, J. C. Huffman, G. Christou, D. N. Hendrickson, *J. Am. Chem. Soc.* **1991**, *113*, 3012.

[S-6] J. K. McCusker, C. A. Christmas, P. M. Hagen, R. K. Chadha, D. F. Harvey, D. N. Hendrickson, *J. Am. Chem. Soc.* **1991**, *113*, 6114.

[S-7] M. Sheldrick; *SHELXL-97*, Program for crystal structure refinement; University of Göttingen: Germany, **1997**.

[S-8] A. Boultif, D. Louer, *J. Appl. Cryst.* **2004**. *37*, 724.

[S-9] J. Rodriguez-Carvajal, *Physica B* **1993**, *192*, 55.